JOURNAL OF VIROLOGY, Dec. 2002, p. 12233–12241 Vol. 76, No. 23
0022-538X/02/$04.00+0 DOI: 10.1128/JVI.76.23.12233–12241.2002

Regulation of Indoleamine 2,3-Dioxygenase Expression in Simian Immunodeficiency Virus-Infected Monkey Brains†

E. M. E. Burudi, M. Cecilia G. Marcondes, Debbie D. Watry, Michelle Zandonatti, Michael A. Taffe, and Howard S. Fox*

Department of Neuropharmacology, The Scripps Research Institute, La Jolla, California 92037

Received 4 April 2002/Accepted 23 August 2002

The human immunodeficiency virus type 1-associated cognitive-motor disorder, including the AIDS dementia complex, is characterized by brain functional abnormalities that are associated with injury initiated by viral infection of the brain. Indoleamine 2,3-dioxygenase (IDO), the first and rate-limiting enzyme in tryptophan catabolism in extrahepatic tissues, can lead to neurotoxicity through the generation of quinolinic acid and immunosuppression and can alter brain chemistry via depletion of tryptophan. Using the simian immunodeficiency virus (SIV)-infected rhesus macaque model of AIDS, we demonstrate that cells of the macrophage lineage are the main source for expression of IDO in the SIV-infected monkey brain. Animals with SIV encephalitis have the highest levels of IDO mRNA, and the level of IDO correlates with gamma interferon (IFN-γ) and viral load levels. In vitro studies on mouse microglia reveal that IFN-γ is the primary inducer of IDO expression. These findings demonstrate the link between IDO expression, IFN-γ levels, and brain pathology signs observed in neuro-AIDS.

Simian AIDS (sAIDS) is the nonhuman primate equivalent of AIDS in humans and results from infection of Asian macaques with the simian immunodeficiency virus (SIV), highly analogous to human infection with human immunodeficiency virus (HIV). In addition to immune deficiency and the resulting opportunistic infections and malignancy, sAIDS is characterized by motor, cognitive, and behavioral abnormalities during its mid-stage to late stage of infection (29, 36), mimicking the HIV type 1 (HIV-1) cognitive-motor disorder found in humans, also known as the AIDS dementia complex or neuro-AIDS.

In both monkeys and humans, the central nervous system (CNS) disorder is thought to result from indirect mechanisms initiated by viral infection of the brain, resulting in functional and pathological changes occurring in the regions of the brain responsible for integrating these higher functions. Encephalitis can result from HIV and SIV infection, with lesions consisting of multinucleated giant cells, microglia nodules, perivascular cuffing, and astrocytosis (20, 41). However, encephalitis does not strictly correlate with functional abnormalities of the CNS. Other more subtle but significant changes reported include neuronal dendritic loss and dendritic vacuolization (19, 25). Similar to what is found for HIV, analysis of the brains and cerebrospinal fluid (CSF) of SIV-infected monkeys reveals an increased expression of inflammatory cytokines including tumor necrosis factor alpha (TNF-α), gamma interferon (IFN-γ), interleukin-1β (IL-1β), IL-6, and inducible nitric oxide synthase (iNOS) (2, 21) and chemokines including monocyte chemoattractant protein 1 (MCP-1), MCP-3, IFN-γ-inducible protein 10, macrophage-inflammatory protein 1α (MIP-1α), MIP-1β, and RANTES (8, 32). Neurotoxins such as quinolinic acid and peroxynitrite have also been detected in the CSF and brain parenchyma of patients and monkeys with brain inflammation (3, 16, 30)

Previous studies have shown that the severity of neuro-AIDS best correlates with the level of activated macrophages and microglia in the brain as opposed to the level of viral infection (11), although a recent report indicates that a high viral load may indeed correlate with dementia (26). Considering the cytokine milieu in the SIV-infected and inflamed brain and the elevation of activated microglia and macrophages, it is likely that this combination of virus and host factors would lead to increased neurotoxin generation by these cells.

The production of neurotoxins by the host or virus following infection is an important means by which HIV and SIV may cause neurological disease. A potential mechanism for neural damage by cells infected by SIV or HIV in the brain is via the *N*-methyl-D-aspartate (NMDA) receptors, a subtype of glutamate receptor (22). Excessive stimulation of these receptors leads to a cascade of increased neuronal intracellular calcium, increased glutamate release, and overexcitation of neurons, eventually resulting in neuronal damage and death. Increased accumulation of quinolinic acid in the CSF and brain tissue has been reported to be one of the hallmarks of neurological dysfunction in patients with neuro-AIDS and in SIV-infected macaques (5, 14–16, 30, 34). It is thus probable that quinolinic acid, being an excitatory neurotransmitter acting via the NMDA receptor, is a contributing factor to the neuronal dysfunction observed in these cases.

Although macrophages are thought to be the main source of this excitatory neurotoxin, which is generated by oxidative catabolism of tryptophan, endothelial cells and astrocytes have also been shown by in vitro studies to be potential sources. Stimulation of macrophages with lipopolysaccharide (LPS), IFN-γ, or TNF-α leads to increased quinolinic acid production, whereas stimulation with transforming growth factor β2, IL-

* Corresponding author. Mailing address: Department of Neuropharmacology, CVN 8, The Scripps Research Institute, 10550 N. Torrey Pines Rd., La Jolla, CA 92037. Phone: (858) 784-7171. Fax: (858) 784-7296. E-mail: hsfox@scripps.edu.

† Paper 14882-NP from The Scripps Research Institute.

1β, and IL-6 has no apparent effect (9, 35). Furthermore, although viral proteins such as Tat and Nef, as well as platelet-activating factor, are potent inducers of quinolinic acid production in macrophages (35), their mechanisms of action remain unclear.

Indoleamine 2,3-dioxygenase (IDO) is the first and rate-liming enzyme in the generation of quinolinic acid from tryptophan via the kynurenine pathway in extrahepatic tissues (13). In vitro, IDO is shown to be induced in macrophages by IFN-γ, TNF-α, LPS, and CD40 ligand (CD40L) (1, 9), among other stimuli. By depleting the essential amino acid tryptophan, IDO is also thus involved in immune regulation as an inhibitor of T-cell proliferation (18) and in the brain can contribute to serotonin depletion leading to CNS dysfunction (40). Although previous studies have shown increased IDO activity in brain samples from neuro-AIDS patients (31), no detailed examination of its temporal and spatial expression has been performed. We report the regional modulation of IDO in brains of monkeys infected with SIV and its correlation with viral load, IFN-γ expression, and CNS pathology.

MATERIALS AND METHODS

Materials. NG-monoethyl-L-arginine monoacetate (NMM) was obtained from Sigma (St. Louis, Mo.). Sources for antibodies used in immunohistochemistry were as follows: HAM56, MAC387, and glial fibrillary acidic protein (GFAP), Dako (Carpinteria, Calif.); LN3, Zymed (South San Francisco, Calif.); CD3-12, Novocastra (Newcastle-upon-Tyne, United Kingdom); FA2 anti-SIV p27 Gag, produced in our laboratory from a hybridoma provided by the National Institutes of Health AIDS Research and Reference Reagent Program. The CD8-depleting cM-T807 antibody was obtained from the Resource for Primate Lymphocyte-Depleting Monoclonal Antibodies (Beth Israel Deaconess Medical Center, Boston, Mass.). All cytokines were purchased from PeproTech Inc. (Rocky Hill, N.J.); CD40L was obtained from Research Diagnostics Inc. (Flanders, N.J.). Oligonucleotide primers and probes were supplied by Annovis (Aston, Pa.).

Infections. Macaque monkeys (*Macaca mulata*), free of type D simian retroviruses and herpes B virus, were acquired from Charles River (Key Lois, Fla.) and Covance (Alice, Tex.) and prepared for the experiments in accordance with The Scripps Research Institute's Animal Care and Use Committee guidelines.

The animals were divided into three groups. Group A consisted of five uninfected controls (animals 298, 331, 332, 357, and 392); two of these animals received the anti-CD8 antibody treatment described below. The other two groups were infected with SIVmac182, derived from microglia passage of SIVmac251 (38). Animals were inoculated via the saphenous vein with a cryopreserved cell-free SIVmac182 stock (p27 Gag antigen equivalent of 0.9 ng). They were also treated with the anti-CD8 antibody cM-T807 to deplete CD8 cells at different times following SIV inoculation by modifications of the protocol of Schmitz et al. (33). Group B consisted of chronically infected animals that were sacrificed at 21 to 24 months postinoculation (p.i.) without signs or symptoms of simian AIDS due to lack of disease progression (per protocol, with a predetermined criterion of 18 to 24 months p.i. without disease progression). Of the three animals in Group B (animals 290, 291, and 304), animals 290 and 304 were treated with the anti-CD8 antibody on days 462, 465, and 469 p.i., whereas the third (291) was treated on days 210, 213, and 217 p.i. This led to a transient depletion of CD8 cells (recovering to >200 $CD8^+$ cells per μl of blood by 32 days following the final treatment) accompanied by a transient rise in viral load. No progression of disease over time was noted, and animals were later sacrificed at 641 (291), 646 (304), and 723 (290) days following infection. Group C consisted of animals that were treated with the anti-CD8 antibody near the time of infection in order to induce a more rapid disease course, reported to yield a high incidence of encephalitis (43). These four animals (animals 301, 321, 323, and 330) were treated with the anti-CD8 antibody at days 6, 9, and 13 p.i. and developed transient CD8 depletion (recovering to > 200 $CD8^+$ cells per μl of blood by day 45 p.i., 32 days following the final treatment) but had a consistently high viral load until sacrifice. These animals were sacrificed at 93 (323), 101 (301), 108 (321), and 111 (330) days following viral inoculation due to the predetermined criterion of development of symptomatic simian AIDS.

Tissues were acquired following deep anesthesia of the animals with ketamine, xylazine, and pentobarbital and complete vascular perfusion with heparinated phosphate-buffered saline (PBS). Sections were immediately fixed in 10% neutral buffered formalin or preserved in RNA-later (Ambion, Austin, Tex.) for RNA isolation.

Cultured microglia. Microglia was isolated from the brains of monkeys as described previously (24). The cells were plated in a six-well plate in RPMI 1640 containing 10% fetal calf serum, PenStrep, amphotericin B (Fungizone), and 50 ng of macrophage colony-stimulating factor/ml for 7 days at 37°C and 5% CO_2 before use. Purity was determined by incubation with fluorescent dye laurdan-labeled acetylated low-density lipoprotein, followed by examination by fluorescence microscopy, as previous described (21), and was found to be >95%.

To isolate mouse microglia, brains from four newborn mouse pups were triturated in 10 ml cDMEM (Dulbecco's modified Eagle medium with 10% fetal calf serum, PenStrep, and Fungizone) containing trypsin-EDTA and incubated at room temperature for 20 min. To harvest the cells, 40 ml of cDMEM was added and cells were pelleted at 2,000 rpm for 10 min. The cell pellet was reconstituted in 30 ml of cDMEM and plated in two 75-cm^2 flasks at 37°C and 5% CO_2 with media change the next day. After 7 days in culture, the cells were detached in PBS-trypsin-EDTA, harvested in cDMEM, and replated in two plastic 24-well plates in cDMEM containing 50% of the previous culture's medium and 50 ng of macrophage colony-stimulating factor/ml for 7 days before use.

RNA isolation. Monkey brain RNA was isolated by homogenization in Trizol (Gibco, Carlsbad, Calif.), with an additional phenol-chloroform extraction. Mouse brain and microglia RNA were isolated with a Totally RNA kit (Ambion). RNA was reconstituted in diethyl pyrocarbonate (DEPC)-treated water and quantified on a Beckman DU640B spectrophotometer.

Monkey sequences. The human IDO sequence from GenBank was used to design forward (CGGTC TGGTG TATGA AGGGT TCTG) and reverse (CGGAC TGAGG GATTT GACTC TAATG) primers to generate a 216-bp PCR product. cDNA prepared from SIV-infected monkey brain RNA was used as a template. This PCR product was cloned into the pCR 2.1 vector (Invitrogen, Carlsbad, Calif.), transformed into TOP 10F cells (Invitrogen), and sequenced. The associated rhesus monkey IDO sequence and the GenBank rhesus monkey IFN-γ sequence were used to design primers and probes for real-time PCR with the help of the Primer Express software (Applied Biosystems, Foster City, Calif.). The TNF-α primers and probes were adapted from those reported for humans (4) with a single base change in the forward primer to account for a difference between the rhesus monkey and human sequences based on the GenBank rhesus monkey TNF-α sequences. The 18S and SIV primers and probes were those previously reported (10, 17). The probes were labeled with 6-carboxyfluorescein (FAM) as the fluorochrome and tetramethylrhodamine (TAMRA) as the quencher. All primers and probes were purified by polyacrylamide gel electrophoresis and double high-pressure liquid chromatography, respectively. The sequences and concentrations (micromolar) of the primers and probes used in real-time PCR are shown in Table 1.

RT-PCR. For generation of cDNA, 1 to 2 μg of RNA was incubated with random primers and SuperScript II reverse transcriptase (RT) (Gibco) at 42°C for 1 h, followed by 10 min at 90°C to inactivate the reverse transcription reagents.

Real-time PCR. Lyophilized primers and probes were reconstituted in DEPC-treated water to 100 μM stock. Reactions utilized one Ready-To-Go PCR bead (Amersham-Pharmacia Biotech Inc., Piscataway, N.J.) in 25 μl, yielding 1.5 U of *Taq* DNA polymerase, 10 mM Tris-HCl, 50 mM KCl, 1.5 mM $MgCl_2$, and 200 μM (each) deoxynucleoside triphosphate; reaction mixtures were brought to a final concentration of 3.5 mM $MgCl_2$. Real-time PCR was performed on a Smart Cycler real-time machine (Cepheid, Sunnyvale, Calif.) using Smart Cycler tubes from Fisher (Sunnyvale, Calif.). Each assay was optimized by titrating a range of primer and probe concentrations and determining their cycle threshold (CT) values. The primer-probe combinations that gave the lowest CT were used for the final analysis. Additionally, a dilutional analysis of the samples indicated a correlation coefficient for concentration and a CT of 0.99.

To perform the quantitative real-time PCR, the RT product was diluted with an equal volume of DEPC-treated water and 7 μl was used for IDO, SIV, TNF-α, and IFN-γ, while 2 μl was used for analysis of 18S in a 25-μl reaction mixture in triplicate. The reaction was run in the Smart Cycler at an initial 95°C for 90 s and then at 95°C for 15 s and 62.5°C for 45 s for 45 cycles. The optic signal was recorded at the end of every 62.5°C annealing/extension step.

Data analysis. For computing the relative amounts of IDO, IFN-γ, TNF-α, and SIV mRNA in the samples, the average CT of the primary signal for 18S was subtracted from that for IDO, IFN-γ, TNF-α, and SIV to give changes in CT (dCTs). A baseline dCT of 25 was subtracted from these dCTs, and the resultant values were multiplied by −1 to get the difference in the dCTs (ddCT, $\log_2$ relative units) used here as the measure of mRNA concentration. The normal-

ization of IDO with 18S controls for variation in efficiency of RNA isolation, possible differences in amounts of starting mRNA, and RT efficiency.

For statistical analysis, the ddCT values were used. Comparisons between groups were analyzed by one-way analysis of variance, followed, when a significant difference was found, by Student-Newman-Keuls tests for comparisons of data among the groups. Results were deemed significant at a P value <0.05. The strength of association between two variables (IDO and cytokine or virus levels) was determined by using the Pearson product-moment correlation coefficient (r).

Immunohistochemistry. Formalin-fixed tissue sections were embedded in paraffin wax. Six-micrometer sections were treated with xylene to remove the paraffin and rehydrated for 3 min each in 100, 95, 75, and 50% ethanol followed by PBS. Endogenous peroxidase activity was quenched by treatment with 0.3% hydrogen peroxide in methanol. The sections were then washed in PBS before treatment with 0.01 M sodium citrate, pH 6.39, at 104°C. Nonspecific binding was blocked in casein before an overnight staining with primary antibody at 4°C. A biotinylated secondary antibody (Vector Laboratories, Burlingame, Calif.) was used at 1:100, followed by Histostain-Plus streptavidin peroxidase conjugate (Zymed), and visualized with the VIP chromogen in accordance with the manufacturer's (Vector) instructions. The slides were then counterstained with methyl green, dehydrated, and mounted. A minimum of four level sections were stained with each antibody and examined microscopically. The staining patterns and histopathologies on the level sections, as well as on at least 12 sections from other regions of the brain, were similar.

In situ hybridization. The IDO cDNA described above was inserted in the pBS SKII plasmid and used to develop a riboprobe labeled with ^{35}S-UTP according to the manufacturer's instructions (Stratagene). Six-micrometer-thick formalin-fixed, paraffin-embedded brain sections were dewaxed, hydrated, and treated with citrate in heat as described above. Following washes in 0.5× SSC (1× SSC is 0.15 M NaCl plus 0.015 M sodium citrate), the sections were prehybridized for 1 to 3 h at 42 to 46°C in a buffer containing 50% formamide, 0.3 M NaCl, 20 mM Tris (pH 8), 5 mM EDTA, 1× Denhardt's solution, 10 mM dithiothreitol, and 10% dextran sulfate in DEPC water. Subsequently, they were hybridized with 3×10^6 cpm of probe in the same buffer at 42 to 46°C overnight. Following washes and RNase treatment, immunohistochemical staining was done on selected slides as described above. The slides were vacuum dried overnight and coated with NTB2 nuclear emulsion in accordance with the manufacturer's instructions (Eastman Kodak, Rochester, N.Y.). Following a 1- to 2-week exposure, the slides were developed, counterstained with methyl green, and mounted. Antisense probes were used to detect the specific RNAs, and sense strand probes were used for controls. Triplicate sections from at least three different regions of the brain were examined. Analysis for IFN-γ expression in the brain was similarly performed with the probe previously described (21).

Photomicroscopy. Representative microscopic fields were captured with a Spot RT Color charge-coupled device camera with the assistance of Spot RT software (Spot Diagnostic Instruments, Inc., Sterling Heights, Mich.) and an Optiphot microscope (Nikon Instruments, Inc., Melville, N.Y.).

Nucleotide sequence accession number. The GenBank accession number for the 216-bp PCR product is AF533656.

RESULTS

IDO expression in microglia. To investigate the regulation of IDO mRNA expression in microglia, initial studies of mouse microglia isolated from newborn pups were performed. In cultured mouse microglia, addition of IFN-γ led to a significant induction of IDO (Fig. 1a). TNF-α had a small but significant stimulatory effect on IDO expression, which was augmented by IFN-γ (Fig. 1b). LPS had no significant effect on its own and did not alter the level induced by IFN-γ (Fig. 1c). Since nitric oxide, formed via the production of iNOS, has been shown to inhibit IDO activity, NMM, an inhibitor of iNOS activity, was added to the cultures. In the mouse microglia cultures NMM had no effect when used alone or in the presence of IFN-γ (Fig. 1d).

Studies on microglia isolated from macaques were then performed. In microglia derived from monkeys, cells from both uninfected and SIV-infected animals were found to express basal levels of IDO mRNA under these culture conditions.

TABLE 1. Sequences of the oligonucleotide primers and probes used in quantitative real-time PCR

RNA target[a]	Sequence (final conen in reaction mixture [μM]) of:		
	Forward primer	Reverse primer	Probe
mIDO	GAGAA AGCCA AGGAA ATTTT TAAGA G (0.66)	GATAT ATGCG GAGAA CGTGG AAA (0.22)	TGCGT GACTT TGTGG ACCCA GACAC (0.24)
rIDO	TGCTT TGACG TCCTG CTGG (0.66)	TTCCT GTGAG CTGGT GGCA (0.22)	ATGCT GCTCA GTTCC CCCAGG GACA (0.24)
rIFN-γ	GCAGA TAATG GAACT CTTTT CTTAG ACA (1.00)	AGGAG ACAAT TTGGC TCTGC AT (1.00)	TTTCT GTCAC TCTCC TCTTT CCAAT TCCTC CAA (0.26)
rTNF-α	ATCTT CTCGA ACCCC AAGTG A (0.80)	CGGTT CAGCC ACTGG AGCT (0.80)	CCCAT GTTGT AGCAA ACCCT CAAGC TGA (0.40)
SIV	GCAGA GGAGG AAATT ACCCA GTAC (0.40)	CAATT TTACC CAGGC ATTTA ATGTT (1.20)	TGTCC ACCTG CCATT AAGCC CGA (0.40)
m/r18S	CGGCT ACCAC ATCCA AGGAA (1.20)	GCTGG AATTA CCGCG GCT (0.40)	TGCTG GCACC AGACT TGCCC TC (0.40)

[a] m, mouse; r, rhesus monkey; m/r, mouse and rhesus monkey.

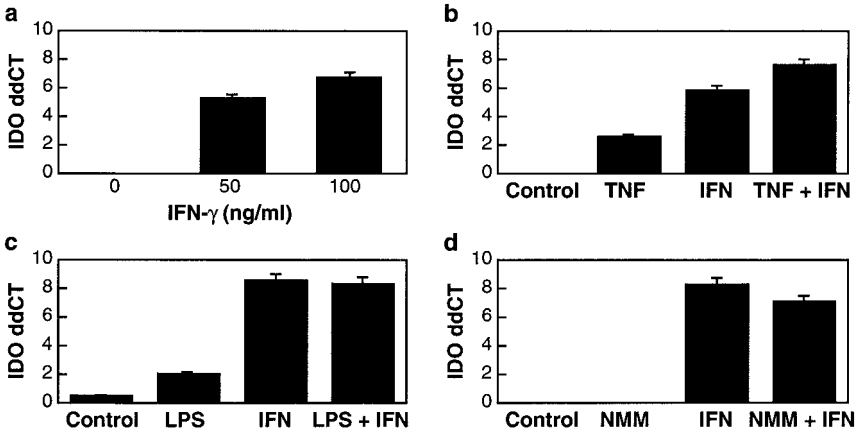

FIG. 1. Modulation of IDO in mouse microglia in vitro. Relative mRNA levels were quantified by real-time RT-PCR. The *y* axis indicates ddCT ($\log_2$ relative units). (a) Cells were stimulated with 0 to 100 ng of IFN-γ/ml for 24 h. IFN-γ induces and significantly up-regulates the expression of IDO in a concentration-dependent manner. (b) Cells were stimulated with 200 ng of TNF-α/ml alone and in combination with 100 ng of IFN-γ/ml for 24 h. IDO expression analysis showed significant low-level induction by TNF-α alone; when TNF-α was combined with IFN-γ, there was a complementary effect. (c) Cells were stimulated with LPS (100 ng/ml), with and without IFN-γ (100 ng/ml) for 24 h. LPS alone resulted in minimal induction of IDO and did not alter the IFN-γ IDO induction. (d) Cells were treated with NMM (100 μm) with and without IFN-γ (100 ng/ml) for 24 h. NMM had no significant effect alone or on IFN-γ-induced IDO expression. For all the experiments, control cells were cultured without the indicated agents.

This basal level was significantly up-regulated by IFN-γ (Fig. 2). CD40L treatment of the microglia did not significantly alter IDO levels in the presence of IFN-γ (Fig. 2). In the monkey microglia, TNF-α had a minimal up-regulating effect, whereas NMM was found to have no significant effect, either alone or in combination with IFN-γ (data not shown).

IDO expression in the brain. Monkeys infected with SIV were evaluated for the expression of IDO in the brain. RNA samples from three groups of monkeys (uninfected, chronically infected but without AIDS at 21 to 24 months p.i., and a group that rapidly progressed to AIDS at 3 to 4 months p.i.) were analyzed for IDO mRNA expression. Since our previous work had indicated that SIV was most consistently detectable in cerebellar RNA (24), cerebellar samples from the groups were compared. All brain tissues from uninfected (group A) monkeys had undetectable levels of IDO mRNA. The animals in the chronic stage of infection (group B) had a significantly up-regulated mean relative level of IDO mRNA of 324 ($2^{8.34}$). Monkeys that were infected with SIV and that rapidly developed AIDS (group C animals) had the highest level of IDO transcripts, with a mean relative level of 8,135 ($2^{12.99}$) (Fig. 3A), significantly different from levels for both uninfected (group A) and chronically infected (group B) animals.

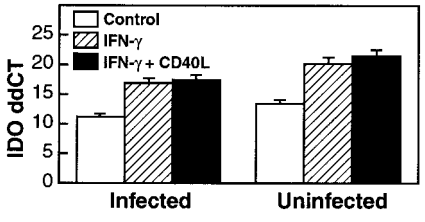

FIG. 2. In vitro modulation of IDO in monkey microglia. Relative mRNA levels were quantified by real-time RT-PCR. The *y* axis indicates ddCT ($\log_2$ relative units). Cells isolated from infected or uninfected monkey brains were stimulated with IFN-γ (100 ng/ml), with and without CD40L (500 ng/ml), for 24 h. IFN-γ treatment resulted in significant IDO induction, which was not significantly altered by CD40L. Control cells were cultured without inducing agents.

Brain viral load. To determine whether the regulation of IDO observed in monkeys infected with SIV was attributable to observed differences in viral load levels in the tissues, the same cerebellar samples were analyzed for SIV RNA. Similar to IDO levels, relative SIV levels in group C, monkeys with AIDS, were significantly higher (244,589; $2^{17.9}$) than those in the group B animals sacrificed during the chronic infection (23; $2^{4.54}$); the uninfected monkeys (group A) were negative for the viral RNA as expected (Fig. 3B).

Brain IFN-γ levels. Following the observation that IFN-γ is the most potent endogenous inducer of IDO expression in microglia, as well as in macrophages and astrocytes in vitro (data not shown), we determined the levels and regulation of IFN-γ transcripts in the same samples in order to understand the mechanism by which viral infection may be causing the up-regulation of IDO. All infected animals had higher levels of IFN-γ mRNA than the uninfected controls. Control group A had no detectable amount of IFN-γ, whereas animals in the chronic stage of infection (group B) had a low level of IFN-γ transcripts (1.4; $2^{0.51}$). The highest levels (41.6; $2^{5.38}$) were again observed in animals with rapidly progressive AIDS (group C) (Fig. 3C); these were significantly different from those for the other two groups. Thus it was evident that there is also a correlation between the amount of IFN-γ and the generation of IDO in the brain, suggesting that IFN-γ is a major potent IDO inducer in SIV infection in the brain.

Brain TNF-α levels. One other immunomodulant found to have a regulating effect on IDO expression is TNF-α. To determine whether TNF-α has a role in the regulation of IDO in the brains of SIV-infected monkeys, we assayed for its transcripts in the same brain samples used for the other molecules. TNF-α mRNA was found in all groups, with the uninfected (group A) animals having the lowest mean level (60; $2^{5.91}$); higher levels were seen in the chronically infected (group B)

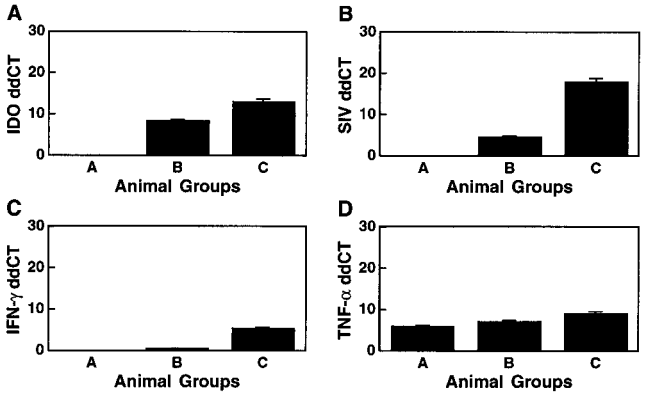

FIG. 3. Cerebellar RNA levels of IDO, SIV, IFN-γ, and TNF-α. Relative mRNA levels were quantified by real-time RT-PCR. The *y* axis indicates ddCT ($\log_2$ relative units). IDO (A), SIV (B), IFN-γ (C), and TNF-α (D) expression levels are significantly higher in animals with rapidly progressive AIDS (group C) than in chronically infected animals (group B). No expression is found in controls (group A).

animals (135; $2^{7.08}$), and the highest levels, significantly different from those for the other two groups, were found in the group C animals (508; $2^{8.99}$), which had rapidly progressive AIDS (Fig. 3D).

SIV-induced pathology. To better characterize the differences between the groups, cerebellar sections were examined by immunohistochemistry with HAM56 (macrophage marker), MAC387 (newly immigrated activated macrophages), LN3 (HLA-DR; on activated endothelial and immune cells), and CD3-12 (for T cells) (Fig. 4). Examination of sections from control animals (group A), such as animal 298, for HAM56-reactive cells revealed only a few faintly staining perivascular cells, dispersed largely in the white matter. No MAC387-reactive or CD3-12-reactive cells were found, and only rare LN3-reactive blood vessels were present. Chronically infected animals (group B, such as animal 291) had HAM56- and LN3-positive micronodules scattered within the white matter. Small foci of CD3-12-positive T cells could be found. LN3-reactive blood vessels were also present. However, in the group C animals, which developed rapidly progressive sAIDS, two distinct patterns of pathology were found. In animals 301, 321, and 323, frank SIV encephalitis (SIVE) was present, including numerous microglia and macrophage nodules, multinucleate giant cells, and perivascular macrophages, predominately in the white matter, which were HAM56 positive, as exemplified by animal 321. MAC387-reactive cells were detected in the same lesions, although the positive cells were less numerous than HAM56-positive cells. CD3-12-positive T cells were also found, largely within or near the nodules. Major histocompatibility complex class II expression, as determined by LN3 staining, was found in nodules, blood vessels, and cells (with the morphology of microglia) in the white (quite intense) and gray matter (less intense). In contrast, animal 330 had foci of perivascular and infiltrating HAM56-positive macrophages but no nodules or giant cells. MAC387 reactivity was not seen. Scattered CD3-12-positive T cells were found in the parenchyma. LN3 reactivity was found focally on microglial cells in the white matter, endothelial cells, and a few perivascular macrophages.

Correlation between virus, cytokines, and IDO. The data above reveal that the animals in group C had higher levels of IDO, SIV, IFN-γ, and TNF-α RNA and more-severe histopathology than those in group B (and similarly for group B compared to group A). The three animals in group C (301, 321, and 323) with SIVE also exhibited higher RNA levels of all measured molecules than the fourth animal (330) in the group, which had less-distinct histopathology. To better discern the relationship between IDO and SIV, IFN-γ, and TNF-α levels in the brain in the setting of SIVE, four other regions of the brain (in addition to the cerebellar samples above; frontal cortex, occipital cortex, midbrain, and hippocampus) from the three animals in group C with SIVE were analyzed for levels of RNA of the above molecules. Examination of the association between IDO levels and the other molecules in these five regions revealed that the strongest correlation was between IDO and IFN-γ mRNA levels (Fig. 5).

Identification of IDO- and IFN-γ-expressing cells. Immunohistochemistry for macrophage markers, the SIV Gag protein, and GFAP, combined with in situ hybridization for IDO, was then performed to discern the origin of IDO in the brains of animals with SIVE. IDO expression was found concentrated in microglia and macrophage nodules, in which a high fraction of the cells were infected with SIV (Fig. 6). IDO expression was not detected in astrocytes or in HAM56-negative cells of the brain. Separate in situ hybridization for IFN-γ performed on brain sections showed individual cells positive for IFN-γ mRNA in the same nodules found to express high levels of IDO (Fig. 7). Similar examination of the brain of animal 330 revealed a focus of IDO signal over a small cluster of macrophages, whereas no signal was found for IFN-γ; group A and B animals were negative for both molecules (data not shown).

DISCUSSION

In this study, we demonstrate that the up-regulation of IDO in the brains of SIV-infected monkeys is dependent on the stage of infection and that the highest levels occur in animals with SIVE. IFN-γ is similarly up-regulated in the brain tissues of these animals, and this coincides with high viral levels. In vitro, IFN-γ is shown to be a major inducer of IDO expression in microglia.

The development of neuro-AIDS in humans and CNS functional abnormalities in SIV-infected monkeys has been shown to be part of the sequel of HIV and SIV infection in humans and monkeys, respectively. This is thought to be a result of injury to brain neurons caused indirectly by the viral infection. One of the mechanisms by which this is thought to occur is through overexcitation of the NMDA receptors by quinolinic acid. Quinolinic acid, generated by oxidative degradation of tryptophan via the kynurenine pathway, has previously been reported to accumulate in CSF and brain tissue of SIV-infected monkeys and HIV-infected humans (5, 14–16, 30, 34).

To elucidate the role of this pathway in the observed CNS abnormalities, we sought to determine the regulation of IDO, the first and rate-limiting enzyme in the generation of quinolinic acid. The level of IDO transcripts in infected animals was higher than that in uninfected animals, and the up-regulation was most significant in animals manifesting SIVE. The parallel expression of IDO and the viral load levels in the brain ob-

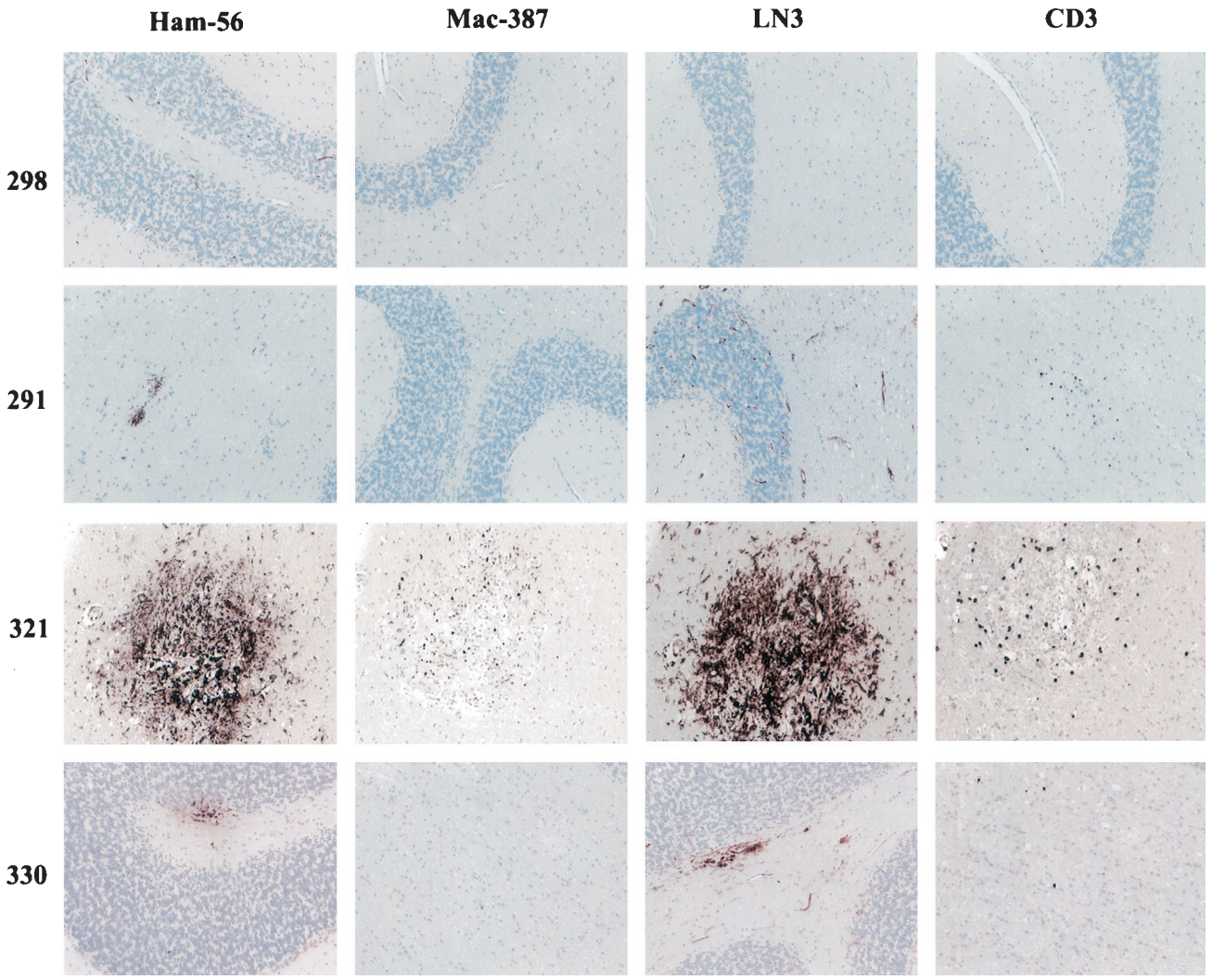

FIG. 4. Immunohistochemical staining for HAM56, MAC387, LN3, and CD-3-12 of cerebellar brain sections from control and SIV-infected monkeys. The two groups of SIV-infected animals manifested different patterns of CNS pathology. Uninfected group A animals do not manifest any lesions (e.g., animal 298). Group B animals, with chronic nonprogressive infection, show small nodules of lymphocytes and macrophages (e.g., animal 291). Group C animals, with a rapid disease course, showed encephalitis (three monkeys; e.g., animal 321) or a less severe pathology (one monkey; animal 330). Magnification, ×100.

served in these studies are in agreement with the findings of others on products of the tryptophan-kynurenine pathway (kynurenic and quinolinic acid). It is evident from our studies that the increased levels of these neurotoxins observed in previous studies (5, 14–16, 30, 34) can be linked to an increase in IDO expression.

The levels of viral load in the brain were in tandem with IDO levels and the presence of SIVE. This may indicate the essential role the presence of virus in the brain plays in the stimulation of IDO expression. In vitro studies have revealed that HIV infection of macrophages can itself induce IDO (12). However such induction of IDO is transient and is dependent on production of IFN-γ by the infected macrophages, and HIV infection did not alter the inducibility of IDO by IFN-γ (12).

By far the most potent producers of IFN-γ are activated T cells. Indeed, we have shown that an influx of activated $CD8^+$ T cells, expressing IFN-γ, occurs in the early stage (11 weeks p.i.) of infection (24). Induction of IDO can also be found at this early stage (data not shown), and higher levels are found in other stages, in tandem with increased levels of IFN-γ.

The lower levels of expression of IDO found in the relatively stable phase of infection (chronic, group B) likely reflect the low level of virus in the brain and may also reflect a differential regulation of IL-4, IL-10, and transforming growth factor β, all possible inhibitors of IFN-γ activity (23). Previous studies have shown that IL-4, generated mainly by Th2-like T cells, and TNF-α are elevated in predementia HIV patients, although, later during dementia, IL-4 is down-regulated (39). This may suggest that, even at such early stages of infection, the milieu of cytokines necessary for the down-regulation or inhibition of IFN-γ is present in the brains of patients with HIV.

IFN-γ, considered a major up-regulating agent for IDO, showed a clear correlation with IDO levels in the brain. Moreover, the animals with simian AIDS, high CNS viral load, and

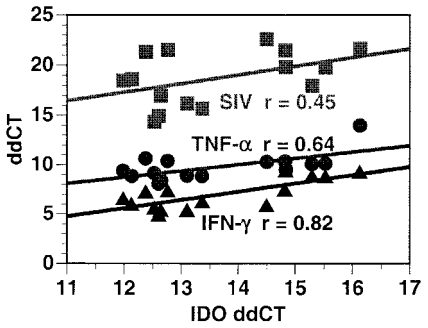

FIG. 5. Scatter chart showing the Pearson product-moment correlation coefficients between IDO expression (*x* axis) and IFN-γ (triangles), TNF-α (circles), and SIV (squares) expression (*y* axis) in brain RNA of animals manifesting SIVE. IDO levels have the strongest correlation with IFN-γ levels, a moderate correlation with TNF-α levels, and the lowest correlation with viral load. Relative RNA levels were quantified by real-time RT-PCR; *x* and *y* axes indicate ddCT ($\log_2$ relative units).

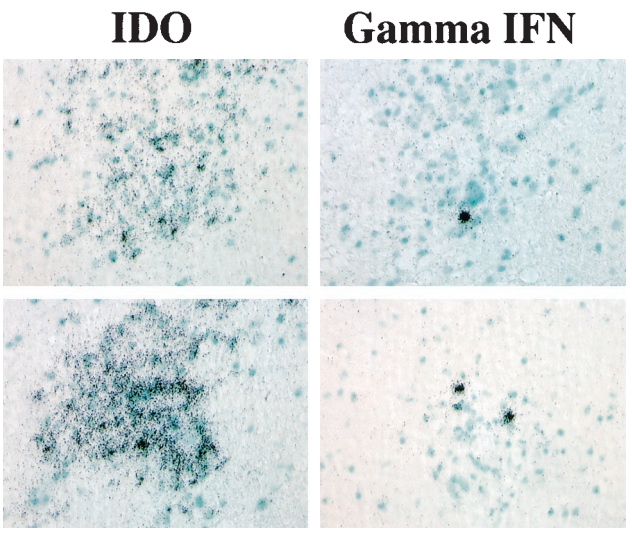

FIG. 7. IFN-γ and IDO expression as examined by in situ hybridization in SIVE. Brain nodules showing high levels of expression of IDO mRNA also contain IFN-γ-expressing cells in the next serial section. Corresponding brain sections from animal 321 are shown. Magnification, ×400.

brain pathology (group C) had significantly higher IFN-γ mRNA levels than those in the chronic stage of infection (group B), whereas no IFN-γ was detected in the uninfected controls (group A). In the animal with AIDS without frank SIVE (330) as well as the three chronically infected animals without significant brain histopathology, lower levels of virus, IFN-γ, and IDO were present. However the levels in some regions of the brain were often just at or below the level of detection, preventing the detailed correlation performed for the animals with SIVE.

We also observed a basal level of TNF-α mRNA expression in the brains of all animals regardless of whether they were infected or not. Whether translational activation (42) is the main mechanism at play in TNF-α production is still open to investigation. Our findings show that TNF-α alone is unable to highly induce IDO in vitro. However, it has been reported that in some glioblastoma cells TNF-α has a synergistic effect when

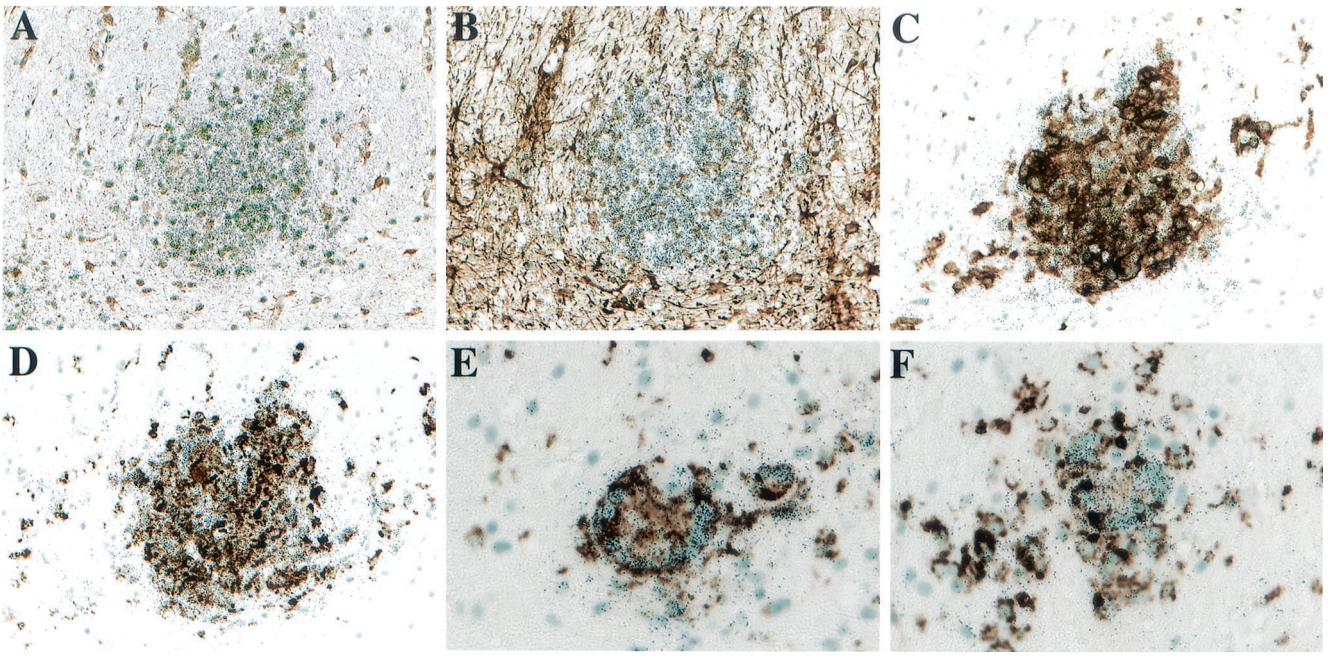

FIG. 6. IDO in situ hybridization (silver grains) in SIVE, combined with immunohistochemistry (brown diaminobenzidine product). (A) IDO mRNA is observed in the nodules largely within the white matter (no primary antibody). (B) Immunohistochemical staining for GFAP reveals no colocalization with astrocytes. (C) Immunohistochemical staining with the FA2 antibody (for SIV Gag) reveals colocalization with SIV-expressing cells. (D to F) Immunohistochemical staining with the HAM56 antibody reveals colocalization with cells of the macrophage lineage. Data from monkeys 321 (A to D; magnification, ×200) and 323 (E and F; magnification, ×400) are shown.

combined with IFN-γ (7) and that the IFN-γ-independent, LPS-induced induction of IDO in gene-disrupted mice may result from the action of TNF-α (9). It is also possible that the role of TNF-α in the brain is facilitated or augmented by other IDO-inducing molecules such as CD40L. Thus, although TNF-α mRNA expression in the brain may not be sufficient to induce IDO expression in vivo, in animals with a high expression of IFN-γ, the increased levels of TNF-α that we observed may accentuate the effect of IFN-γ on IDO up-regulation. These phenomena provide a direct correlation between viral load, induction of IFN-γ, up-regulation of IDO, and the development of SIVE, a sequence of events that could culminate in behavioral, motor, and cognitive abnormalities.

In studies done in our laboratory and others, it has been shown that there is an increase in the number of T cells in the brains of SIV-infected monkeys (20, 24, 36, 37). Specifically, there is a significant increase in $CD8^+$ T cells in the CSF and brain parenchyma. Besides the protective role of these T cells during the viral infection of the brain, it is likely that the T cells in the brain produce IFN-γ, which stimulates the macrophages to make IDO. Here we have found $CD3^+$ T cells in the brains of animals in both group B (chronic infection) and group C (simian AIDS). Although combined in situ hybridization and immunohistochemical staining were not performed, fluorescence-activated cell sorter analysis of brain T-cell populations indicates that $CD8^+$ T cells predominate over $CD4^+$ T cells (by three- to fivefold) in both of these groups, confirming their presence and dominance in the brain (M. C. G. Marcondes, unpublished data). Although T cells are reported to be generators of IDO (6), the levels are quite low, making them unlikely to contribute significantly to the IDO pool emanating from microglia and macrophages. The role of T cells in the generation of IDO via their production of IFN-γ is supported by the high levels of IFN-γ we observe and the very high correlation with IDO levels. Furthermore, we determined that most of the cells generating IDO in the SIVE monkey brains were macrophages and microglial cells. However, it is important that cells staining for the CD3 T-cell marker were also detectable in the brain nodular structures that were positive for virus, IDO, and the macrophage marker HAM56, providing a practical proximity for such signaling.

A concurrent effect of the interplay between T cells and the IDO environment is the immunosuppression of the T cells that results from the tryptophan depletion (27, 28), with the overall consequence of minimizing brain inflammation and reducing T-cell effector functions, allowing the infection to thrive. Subsequently, the T cells may undergo apoptosis if tryptophan is not restored and a second signal from the T-cell receptor (TCR) is not forthcoming (27). Alternatively, the T cells in the arrested stage may enter a state of anergy or return to a resting state. Thus, the microenvironment we expect around these nodules would include high IDO and low tryptophan levels, hence immunosuppressed, anergic, resting and apoptotic T cells (T cells arrested in G_1 phase), and high kynurenic and quinolinic acid levels, and consequently injured and apoptotic neurons. We are currently investigating this hypothesis.

Our findings are consistent with the theory that, following SIV infection, IFN-γ and IDO can be expressed and maintained at palpable levels by the host response to the presence of virus in the brain, and that the magnitude of the effect of this up-regulation and the maintenance of these levels can be tempered by other modulatory factors generated during the virus-host interaction in individual animals. Interestingly, motor skill impairment in SIV-infected animals, even in relatively early stages of infection, was found to correlate with CSF quinolinic acid level (30), necessitating CNS IDO induction (16). Later in disease, with the onset of immunosuppression, increases in CNS macrophages and virus, in the presence of the host response (e.g., IFN-γ), result in higher levels of quinolinic acid (15, 34) due to increased IDO, resulting from high-level production in macrophage and microglial nodules, and its further untoward effects on CNS function.

In conclusion, we have shown that there is a direct correlation between IFN-γ levels, up-regulation of IDO, brain pathology, and viral load in SIV-infected monkey brain. It is conceivable that the induction of IFN-γ following viral entry to the brain induces macrophages and microglia to generate IDO, which in turn leads to increased quinolinic acid levels, resulting in neurotoxicity. Furthermore, the immunosuppression resulting from IDO generation in virus-infected nodules creates a safe haven for further seeding of the virus and persistence of the infection. This may be a major explanation for the behavioral, motor, and cognitive abnormalities observed in SIV-infected monkeys and HIV-infected humans.

ACKNOWLEDGMENTS

We thank Steven Henriksen, Lisa Madden, Keith Reimann, and Jöern Schmitz for their assistance and input into these studies, and we thank Rebecca Mahady for manuscript preparation. The SIVmac p27 hybridoma FA2 from Suganto Sujipto and Preston Marx was obtained through the AIDS Research and Reference Reagent Program, Division of AIDS, NIAID, NIH.

This work was supported by NIH grants MH59468, MH61224, MH61692, MH62261, and RR13150.

REFERENCES

1. **Alberati-Giani, D., P. Ricciardi-Castagnoli, C. Kohler, and A. M. Cesura.** 1996. Regulation of the kynurenine metabolic pathway by interferon-gamma in murine cloned macrophages and microglial cells. J. Neurochem. **66:**996–1004.
2. **Boche, D., E. Khatissian, F. Gray, P. Falanga, L. Montagnier, and B. Hurtrel.** 1999. Viral load and neuropathology in the SIV model. J. Neurovirol. **5:**232–240.
3. **Boven, L. A., L. Gomes, C. Hery, F. Gray, J. Verhoef, P. Portegies, M. Tardieu, and H. S. Nottet.** 1999. Increased peroxynitrite activity in AIDS dementia complex: implications for the neuropathogenesis of HIV-1 infection. J. Immunol. **162:**4319–4327.
4. **Brink, N., M. Szamel, A. R. Young, K. P. Wittern, and J. Bergemann.** 2000. Comparative quantification of IL-1β, IL-10, IL-10r, TNFα and IL-7 mRNA levels in UV-irradiated human skin in vivo. Inflamm. Res. **49:**290–296.
5. **Coe, C. L., T. M. Reyes, C. D. Pauza, and J. F. Reinhard, Jr.** 1997. Quinolinic acid and lymphocyte subsets in the intrathecal compartment as biomarkers of SIV infection and simian AIDS. AIDS Res. Hum. Retrovir. **13:**891–897.
6. **Curreli, S., F. Romerio, P. Mirandola, P. Barion, K. Bemis, and D. Zella.** 2001. Human primary $CD4^+$ T cells activated in the presence of IFN-alpha 2b express functional indoleamine 2,3-dioxygenase. J. Interferon Cytokine Res. **21:**431–437.
7. **Daubener, W., C. Remscheid, S. Nockemann, K. Pilz, S. Seghrouchni, C. Mackenzie, and U. Hadding.** 1996. Anti-parasitic effector mechanisms in human brain tumor cells: role of interferon-gamma and tumor necrosis factor-alpha. Eur. J. Immunol. **26:**487–492.
8. **Fox, H. S., M. R. Weed, S. Huitron-Resendiz, J. Baig, T. F. Horn, P. J. Dailey, N. Bischofberger, and S. J. Henriksen.** 2000. Antiviral treatment normalizes neurophysiological but not movement abnormalities in simian immunodeficiency virus-infected monkeys. J. Clin. Investig. **106:**37–45.
9. **Fujigaki, S., K. Saito, K. Sekikawa, S. Tone, O. Takikawa, H. Fujii, H. Wada, A. Noma, and M. Seishima.** 2001. Lipopolysaccharide induction of indoleam-

ine 2,3-dioxygenase is mediated dominantly by an IFN-gamma-independent mechanism. Eur. J. Immunol. **31:**2313–2318.
10. **Gerard, C. J., L. M. Andrejka, and R. A. Macina.** 2000. Mitochondrial ATP synthase 6 as an endogenous control in the quantitative RT-PCR analysis of clinical cancer samples. Mol. Diagn. **5:**39–46.
11. **Glass, J. D., H. Fedor, S. L. Wesselingh, and J. C. McArthur.** 1995. Immunocytochemical quantitation of human immunodeficiency virus in the brain: correlations with dementia. Ann. Neurol. **38:**755–762.
12. **Grant, R. S., H. Naif, S. J. Thuruthyil, N. Nasr, T. Littlejohn, O. Takikawa, and V. Kapoor.** 2000. Induction of indolamine 2,3-dioxygenase in primary human macrophages by human immunodeficiency virus type 1 is strain dependent. J. Virol. **74:**4110–4115.
13. **Heyes, M. P., C. Y. Chen, E. O. Major, and K. Saito.** 1997. Different kynurenine pathway enzymes limit quinolinic acid formation by various human cell types. Biochem. J. **326:**351–356.
14. **Heyes, M. P., R. J. Ellis, L. Ryan, M. E. Childers, I. Grant, T. Wolfson, S. Archibald, and T. L. Jernigan.** 2001. Elevated cerebrospinal fluid quinolinic acid levels are associated with region-specific cerebral volume loss in HIV infection. Brain **124:**1033–1042.
15. **Heyes, M. P., K. Saito, J. S. Crowley, L. E. Davis, M. A. Demitrack, M. Der, L. A. Dilling, J. Elia, M. J. Kruesi, A. Lackner, et al.** 1992. Quinolinic acid and kynurenine pathway metabolism in inflammatory and non-inflammatory neurological disease. Brain **115:**1249–1273.
16. **Heyes, M. P., K. Saito, A. Lackner, C. A. Wiley, C. L. Achim, and S. P. Markey.** 1998. Sources of the neurotoxin quinolinic acid in the brain of HIV-1-infected patients and retrovirus-infected macaques. FASEB J. **12:**881–896.
17. **Hofmann-Lehmann, R., R. K. Swenerton, V. Liska, C. M. Leutenegger, H. Lutz, H. M. McClure, and R. M. Ruprecht.** 2000. Sensitive and robust one-tube real-time reverse transcriptase-polymerase chain reaction to quantify SIV RNA load: comparison of one- versus two-enzyme systems. AIDS Res. Hum. Retrovir. **16:**1247–1257.
18. **Hwu, P., M. X. Du, R. Lapointe, M. Do, M. W. Taylor, and H. A. Young.** 2000. Indoleamine 2,3-dioxygenase production by human dendritic cells results in the inhibition of T cell proliferation. J. Immunol. **164:**3596–3599.
19. **Kure, K., K. M. Weidenheim, W. D. Lyman, and D. W. Dickson.** 1990. Morphology and distribution of HIV-1 gp41-positive microglia in subacute AIDS encephalitis. Pattern of involvement resembling a multisystem degeneration. Acta Neuropathol. **80:**393–400.
20. **Lackner, A. A., M. O. Smith, R. J. Munn, D. J. Martfeld, M. B. Gardner, P. A. Marx, and S. Dandekar.** 1991. Localization of simian immunodeficiency virus in the central nervous system of rhesus monkeys. Am. J. Pathol. **139:**609–621.
21. **Lane, T. E., M. J. Buchmeier, D. D. Watry, and H. S. Fox.** 1996. Expression of inflammatory cytokines and inducible nitric oxide synthase in brains of SIV-infected rhesus monkeys: applications to HIV-induced central nervous system disease. Mol. Med. **2:**27–37.
22. **Lipton, S. A., and H. E. Gendelman.** 1995. Seminars in medicine of the Beth Israel Hospital, Boston. Dementia associated with the acquired immunodeficiency syndrome. N. Engl. J. Med. **332:**934–940.
23. **MacKenzie, C. R., R. G. Gonzalez, E. Kniep, S. Roch, and W. Daubener.** 1999. Cytokine-mediated regulation of interferon-gamma-induced IDO activation. Adv. Exp. Med. Biol. **467:**533–539.
24. **Marcondes, M. C., E. M. Burudi, S. Huitron-Resendiz, M. Sanchez-Alavez, D. Watry, M. Zandonatti, S. J. Henriksen, and H. S. Fox.** 2001. Highly activated $CD8^+$ T cells in the brain correlate with early central nervous system dysfunction in simian immunodeficiency virus infection. J. Immunol. **167:**5429–5438.
25. **Masliah, E., R. K. Heaton, T. D. Marcotte, R. J. Ellis, C. A. Wiley, M. Mallory, C. L. Achim, J. A. McCutchan, J. A. Nelson, J. H. Atkinson, I. Grant, et al.** 1997. Dendritic injury is a pathological substrate for human immunodeficiency virus-related cognitive disorders. Ann. Neurol. **42:**963–972.
26. **McClernon, D. R., R. Lanier, S. Gartner, P. Feaser, C. A. Pardo, M. St Clair, Q. Liao, and J. C. McArthur.** 2001. HIV in the brain: RNA levels and patterns of zidovudine resistance. Neurology **57:**1396–1401.
27. **Munn, D. H., J. Pressey, A. C. Beall, R. Hudes, and M. R. Alderson.** 1996. Selective activation-induced apoptosis of peripheral T cells imposed by macrophages. A potential mechanism of antigen-specific peripheral lymphocyte deletion. J. Immunol. **156:**523–532.
28. **Munn, D. H., M. Zhou, J. T. Attwood, I. Bondarev, S. J. Conway, B. Marshall, C. Brown, and A. L. Mellor.** 1998. Prevention of allogeneic fetal rejection by tryptophan catabolism. Science **281:**1191–1193.
29. **Murray, E. A., D. M. Rausch, J. Lendvay, L. R. Sharer, and L. E. Eiden.** 1992. Cognitive and motor impairments associated with SIV infection in rhesus monkeys. Science **255:**1246–1249.
30. **Rausch, D. M., M. P. Heyes, E. A. Murray, J. Lendvay, L. R. Sharer, J. M. Ward, S. Rehm, D. Nohr, E. Weihe, and L. E. Eiden.** 1994. Cytopathologic and neurochemical correlates of progression to motor/cognitive impairment in SIV-infected rhesus monkeys. J. Neuropathol. Exp. Neurol. **53:**165–175.
31. **Sardar, A. M., and G. P. Reynolds.** 1995. Frontal cortex indoleamine-2,3-dioxygenase activity is increased in HIV-1-associated dementia. Neurosci. Lett. **187:**9–12.
32. **Sasseville, V. G., M. M. Smith, C. R. Mackay, D. R. Pauley, K. G. Mansfield, D. J. Ringler, and A. A. Lackner.** 1996. Chemokine expression in simian immunodeficiency virus-induced AIDS encephalitis. Am. J. Pathol. **149:**1459–1467.
33. **Schmitz, J. E., M. A. Simon, M. J. Kuroda, M. A. Lifton, M. W. Ollert, C. W. Vogel, P. Racz, K. Tenner-Racz, B. J. Scallon, M. Dalesandro, J. Ghrayeb, E. P. Rieber, V. G. Sasseville, and K. A. Reimann.** 1999. A nonhuman primate model for the selective elimination of $CD8^+$ lymphocytes using a mouse-human chimeric monoclonal antibody. Am. J. Pathol. **154:**1923–1932.
34. **Sei, S., K. Saito, S. K. Stewart, J. S. Crowley, P. Brouwers, D. E. Kleiner, D. A. Katz, P. A. Pizzo, and M. P. Heyes.** 1995. Increased human immunodeficiency virus (HIV) type 1 DNA content and quinolinic acid concentration in brain tissues from patients with HIV encephalopathy. J. Infect. Dis. **172:**638–647.
35. **Smith, D. G., G. J. Guillemin, L. Pemberton, S. Kerr, A. Nath, G. A. Smythe, and B. J. Brew.** 2001. Quinolinic acid is produced by macrophages stimulated by platelet activating factor, Nef and Tat. J. Neurovirol. **7:**56–60.
36. **Sopper, S., U. Sauer, S. Hemm, M. Demuth, J. Muller, C. Stahl-Hennig, G. Hunsmann, V. ter Meulen, and R. Dorries.** 1998. Protective role of the virus-specific immune response for development of severe neurologic signs in simian immunodeficiency virus-infected macaques. J. Virol. **72:**9940–9947.
37. **von Herrath, M., M. B. Oldstone, and H. S. Fox.** 1995. Simian immunodeficiency virus (SIV)-specific CTL in cerebrospinal fluid and brains of SIV-infected rhesus macaques. J. Immunol. **154:**5582–5589.
38. **Watry, D., T. E. Lane, M. Streb, and H. S. Fox.** 1995. Transfer of neuropathogenic simian immunodeficiency virus with naturally infected microglia. Am. J. Pathol. **146:**914–923.
39. **Wesselingh, S. L., C. Power, J. D. Glass, W. R. Tyor, J. C. McArthur, J. M. Farber, J. W. Griffin, and D. E. Griffin.** 1993. Intracerebral cytokine messenger RNA expression in acquired immunodeficiency syndrome dementia. Ann. Neurol. **33:**576–582.
40. **Widner, B., M. Ledochowski, and D. Fuchs.** 2000. Interferon-gamma-induced tryptophan degradation: neuropsychiatric and immunological consequences. Curr. Drug Metab. **1:**193–204.
41. **Wiley, C. A., E. Masliah, M. Morey, C. Lemere, R. DeTeresa, M. Grafe, L. Hansen, and R. Terry.** 1991. Neocortical damage during HIV infection. Ann. Neurol. **29:**651–657.
42. **Willeaume, V., V. Kruys, T. Mijatovic, and G. Huez.** 1995. Tumor necrosis factor-alpha production induced by viruses and by lipopolysaccharides in macrophages: similarities and differences. J. Inflamm. **46:**1–12.
43. **Williams, K., X. Alvarez, and A. A. Lackner.** 2001. Central nervous system perivascular cells are immunoregulatory cells that connect the CNS with the peripheral immune system. Glia **36:**156–164.